Electronic Supplement to: Low friction along the high slip patch of the 2011 Mw 9.0 Tohoku-Oki earthquake required from the wedge structure and extensional splay faults.

N. Cubas[1], J.P. Avouac,[1], Y.M. Leroy[2], and A. Pons[2]

[1]Tectonics Observatory, Division of Geological and Planetary Sciences, California Institute of Technology, Pasadena, California, USA.
[2]Laboratoire de Géologie, CNRS, Ecole Normale Supérieure, Paris, France.

1 Introduction

The objective of this Electronic Supplement is to present in a concise manner the kinematic approach of limit analysis for fluid saturated media as proposed in details by Leroy and Pons (2012). The limit analysis approach [Chandrasekharaiah and Debnath, 1994; Salençon, 2002] is based on the principle of virtual powers and the theorem of maximum rock strength [Maillot and Leroy, 2006]. The method investigates all possible collapse mechanisms as a function of the frictional properties and selects the optimal one leading to the least upper bound to the tectonic force. The method has previously been applied to retrieve frictional properties of accretionary prism faults [Cubas et al., 2008; Souloumiac et al., 2009; Pons et al., 2013; Cubas et al., subm.a] and has been validated quantitatively from comparison with analogue sandbox experiments [Cubas et al., subm.b]. In this study, the Coulomb criterion is used for the maximum rock strength. The upper bounds to the tectonic force for two of the collapse mechanisms used in the main text are presented.

2 Collapse Mechanism and main objective of the kinematic approach

The starting point of the kinematic approach of limit analysis is the concept of collapse mechanism and two such mechanisms considered in the main text, as shown in Figure 3, are reproduced in Figure 1 of this supplement.

The first collapse mechanism assumes that the whole décollement is activated, although the sections AG and GB have two different velocities. The velocity of the inner section is dictated by the displacement of the back wall AC. The velocity of the frontal region is an outcome of the analysis as well as the orientation of the single fault GE. This fault is normal or reverse depending on the difference in velocity between the two regions. This first collapse mechanism is relevant for a super-critical wedge in the sense of Dahlen [1984] since the whole décollement is activated. Note that this first collapse mechanism should be seen as an example of the various single-fault mechanisms considered in the main text.

The second collapse mechanism requires only partial activation of the décollement from point A to point G. Two faults are rooting at this last point and correspond to the onset of a thrust fold. The outcome of the analysis is the dip of these two faults.

The position of point G, common to the two mechanisms, is set at the termination of the internal section of the décollement.

The benefit of the kinematic approach of limit analysis is to determine upper bounds to the unknown force applied at the back-wall to activate these two mechanisms. The free geometrical parameters are determined to minimize the bounds and each collapse mechanism is optimized to get the minimized upper bound. The

theorem of limit analysis states that the actual force cannot exceed the least of the two minimized upper bounds. It is for that reason that the collapse mechanism corresponding to the least upper bound is proposed as the dominant mode of the wedge deformation. The next section of this ES defines the framework of the kinematic approach leading to this finding.

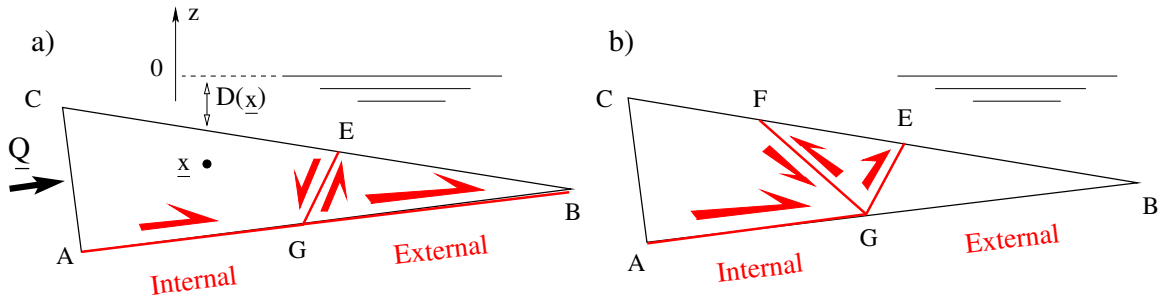

Figure 1: The two collapse mechanisms considered consist of the total or the partial activation of the décollement and the presence of a single fault or a conjugate set of faults rooting at the same point on the décollement and typical of a thrust fold, a) and b), respectively.

3 Kinematic approach

3.1 Theorem of effective virtual powers

The following weak expression of mechanical equilibrium is our starting point:

$$\mathcal{P}_{\text{ext}}(\hat{\underline{U}}) = \mathcal{P}_{\text{int}}(\hat{\underline{U}}) \quad \forall \quad \hat{\underline{U}}\, KA\,. \tag{1}$$

It does not account for inertia and states the equality between the internal and the external powers. This theorem of virtual powers is valid for any kinematically admissible (KA) velocity field. Any velocity field, and not just the exact unknown one, is KA as long as it vanishes on the portion of the boundary where the displacements are prescribed. For example, for our two collapse mechanisms in Figure 1, the velocity of the subducting plate is set to zero with respect to the advancing back wall. Each region of the wedge, say regions $AGEC$ and GBE for the first collapse mechanism are assigned constant velocity resulting in velocity discontinuity along the décollement and the single internal fault. This velocity field is KA and said to be virtual because it does not correspond to the exact, unknown field. It is for that reason that these KA fields are noted with a superposed hat.

The internal power in (1) is defined by

$$\mathcal{P}_{\text{int}}(\hat{\underline{U}}) = \int_{\Omega_t} \underline{\underline{\sigma}} : \hat{\underline{\underline{d}}}\, dV + \int_{\Sigma_U} \underline{T} \cdot \hat{\underline{J}}\, dS\,. \tag{2}$$

It has two terms, the first corresponding to the power of the stress tensor $\underline{\underline{\sigma}}$ by the rate of deformation tensor $\hat{\underline{\underline{d}}}$ (the symmetric part of the virtual velocity field gradient) summed over the domain of the wedge (Ω_t). The second term is the power of the stress vector $\underline{T}$ times the velocity jump $\hat{\underline{J}}$. This velocity jump is the difference across any discontinuity, for example the décollement section AG and the fault GE for the first collapse mechanism[1]. The various discontinuities constitute the set Σ_U over which the power is summed in (2). The external power corresponds to

$$\mathcal{P}_{\text{ext}}(\hat{\underline{U}}) = \int_{\Omega_t} \rho \underline{g} \cdot \hat{\underline{U}}\, dV + \underline{Q} \cdot \hat{\underline{U}}_{AC}\,, \tag{3}$$

and results from the power of the velocity field on the gravity field and on the applied force at the back-wall. The velocity $\hat{\underline{U}}_{AC}$ is the velocity of the wedge material in contact with the back-wall.

[1]The frictional power along the back-wall AC could be accounted for. However, since this contribution is the same for the two collapse mechanisms, it is disregarded in the following discussion.

The effective stress carried by the solid phase of our fluid-saturated continuum is defined by

$$\underline{\underline{\sigma}}' = \underline{\underline{\sigma}} + p\underline{\underline{\delta}}\,, \tag{4}$$

in which p is the pressure of the fluid phase (continuum mechanics convention: compressive stress negative). This pressure is discontinuous across the décollement. The effective stress vector acting on any discontinuity Σ is

$$\underline{T}' = \underline{T} + p_\Sigma \underline{n}\,, \tag{5}$$

where $\underline{n}$ is the normal to the discontinuity pointing towards the plus side. The stress decomposition (4) and (5) introduced in the theorem (1), following Pons and Leroy [2012], results in the theorem of effective virtual powers:

$$\mathcal{P}'_{\text{ext}}(\hat{\underline{V}}) = \mathcal{P}'_{\text{int}}(\hat{\underline{U}}) \quad \forall \quad \hat{\underline{U}}\, KA\,, \tag{6}$$

in which the internal and the external effective powers are defined by

$$\mathcal{P}'_{\text{int}}(\hat{\underline{U}}) = \int_{\Omega_t} \underline{\underline{\sigma}}' : \underline{\underline{\hat{d}}}\, dV + \int_{\Sigma_U} \underline{T}'_\Sigma \cdot \underline{\hat{J}}\, dS\,, \tag{7}$$

and

$$\mathcal{P}'_{\text{ext}}(\hat{\underline{U}}) = \mathcal{P}_{\text{ext}}(\hat{\underline{U}}) + \int_{\Omega_t} p\,\text{div}(\hat{\underline{U}})\, dV + \int_{\Sigma_U} p_\Sigma \underline{n} \cdot \underline{\hat{J}}\, dS\,, \tag{8}$$

respectively. The difference between (6-8) and (1-3) is that in the former set of equations, it is the effective stress tensor or vector which enters the internal power. Furthermore, the pressure field is presented as an external field acting on the virtual volume change or the virtual opening of the discontinuities.

The pressure field needs now to be defined and it is proposed for that purpose to make use of the pressure ratio proposed by Hubbert and Rubey [1959]:

$$\lambda(\underline{x}) = -\frac{p(\underline{x}) - \rho_f g D(\underline{x})}{\sigma(\underline{x}) + \rho_f g D(\underline{x})} \quad \text{with} \quad \sigma(\underline{x}) = \rho g(z + D(\underline{x})) - \rho_f g D(\underline{x})\,, \tag{9}$$

in which ρ_f, ρ, g and $D(\underline{x})$ are the fluid volumetric mass, the saturated solid volumetric mass, the gravity acceleration and the thickness of the fluid above the saturated continuum at point $\underline{x}$, Figure 1a, respectively. The stress σ is negative and corresponds to the pressure resulting from the weight of the column above the point $\underline{x}$ of interest. The z-axis is vertical and directed upwards, Figure 1, so that the gravity vector is $\underline{g} = -g\underline{e}_z$. The pressure p at any point of the medium is thus expressed as

$$p = g[-\lambda\rho z + (\rho_f - \rho\lambda)D]\,, \tag{10}$$

so that the variation of λ between ρ_f/ρ and 1 corresponds to the range of pressure between hydrostatic and lithostatic. Note that the décollement has its own pressure ratio noted λ_D.

The internal power is an unknown since the stress field is unknown. It is for that reason that an upper bound to the internal power is proposed in the next subsection by application of what is referred to in Maillot and Leroy [2006] as the maximum strength theorem.

3.2 Maximum strength theorem

The effective stress vector acting on any discontinuity is decomposed in a normal σ'_n and a tangential component τ in the right-handed basis $\{\underline{n}, \underline{t}\}$ composed of the normal and tangential vector to the discontinuity. These two scalars are within the strength domain

$$G = \{\underline{T}' \,|\, |\tau'| + \tan(\phi)\sigma'_n - C \leq 0\}\,, \tag{11}$$

bounded by the Coulomb criterion defined in terms of the friction angle ϕ and the cohesion C. This set is convex in the space (τ', σ_n) and application of convex analysis [Salençon, 2002] reveals that there is a maximum

to the power $\underline{T}' \cdot \underline{\hat{J}}$ which is called the support function $\pi(\underline{\hat{J}})$. This function for the strength domain defined in (11) reads

$$\begin{array}{ll} \left\{ \begin{array}{ll} \text{case 1}: & 0 \leq \eta < \pi/2 - \phi \\ \text{case 1}': & -\pi/2 + \phi < \eta \leq 0 \end{array} \right. , & \pi(\underline{\hat{J}}) = \hat{J} C \text{cotan}(\phi) \cos(\eta) \,, \\ \text{cases 2 \& 2': } \eta = \pm(\pi/2 - \phi), & \pi(\underline{\hat{J}}) = \hat{J} C \cos\phi \,, \\ \left\{ \begin{array}{ll} \text{case 3}: & \pi/2 - \phi < \eta \leq \pi \\ \text{case 3}': & -\pi \leq \eta < -\pi/2 + \phi \end{array} \right. , & \pi(\underline{\hat{J}}) = +\infty \,, \end{array} \tag{12}$$

in which $\hat{J}$ is the norm of the velocity jump and η the angle between the velocity jump and the normal to the discontinuity. This angle is counted positively anti-clockwise. The structure of this support function has two consequences for our selection of virtual velocity field candidates. Cases 3 and 3' for the orientation of the velocity jump leads to an infinite upper bound of no interest. It is thus necessary to avoid the corresponding ranges of angle and to orientate the velocity jumps according to cases 1,1',2 or 2'. The velocity jumps have thus to be oriented within the cone of the normal to the discontinuity with the half angle $\pi/2 - \phi$. The experience gained from previous works with this theoretical framework without pressure field [Cubas et al., 2008] or including the fluid phase [Pons and Leroy, 2012] is that the velocity jumps are always on the boundary of the cone, corresponding to case 2 and 2' in (12). This conclusion is applied here without any further proof.

The introduction of the support function integrated on the discontinuities constituting the set Σ_U provides the maximum resisting power

$$\mathcal{P}'_{\text{mr}}(\underline{\hat{U}}) = \int_{\Sigma_U} \pi(\underline{\hat{J}}) \, dS \geq \mathcal{P}'_{\text{int}}(\underline{\hat{U}}) \,, \tag{13}$$

which is bounding by above the unknown internal power. Combined with the theorem of effective virtual power in (7), one obtains

$$\mathcal{P}'_{\text{ext}}(\underline{\hat{U}}) \leq \mathcal{P}'_{\text{mr}}(\underline{\hat{U}}) \quad \forall \quad \underline{\hat{U}} \, KA \,, \tag{14}$$

and more specifically:

$$\underline{Q} \cdot \underline{\hat{U}}_{AC} \leq \int_{\Sigma_U} \pi(\underline{\hat{J}}) \, dS - \int_{\Omega_t} \rho \underline{g} \cdot \underline{\hat{U}} \, dV + \int_{\Sigma_U} p_\Sigma \underline{n} \cdot \underline{\hat{J}} \, dS \quad \forall \quad \underline{\hat{U}} \, KA \,, \tag{15}$$

recognizing that the velocity field considered for our two collapse mechanism are divergence free. It is the right-hand side of (15) which provides an upper bound to the force of magnitude Q applied on the back-wall once the velocity field is normalized by the velocity of the wedge material in contact with the surface AC.

4 Virtual velocity fields

The theorem presented in the two previous sections is now applied to the two prototypes of Figure 1. The only technical difficulties in obtaining the upper bound based on (15) is the selection of the virtual velocity field which is now presented.

The velocity of the internal region of the wedge for the first collapse mechanisms has a norm of one for sake of normalization and is oriented at ϕ_{DI} from the décollement dipping at β. This orientation corresponds indeed to case 2 of the support function in (12) since the friction angle is ϕ_{DI} over the internal part of the décollement. This vector reads

$$\underline{\hat{U}}_I = \cos(\beta + \phi_{DI}) \underline{e}_1 + \ sin(\beta + \phi_{DI}) \underline{e}_2 \,. \tag{16}$$

The external region at the wedge front has a velocity oriented at ϕ_{DE} from the décollement but its norm $\hat{U}_E$ is unknown. The difference between the two velocities $\underline{\hat{J}} = \underline{\hat{U}}_E - \underline{\hat{U}}_I$ is the jump over the fault GE dipping at θ, as shown in Figure 1. This jump should be oriented at ϕ (bulk friction angle) from this fault, as illustrated in Figure 2a. The norm of the jump and the norm of the external velocity are dictated from this constraint as seen in the hodogram of Figure 2a. Application of the law of sines to this triangular construction provides

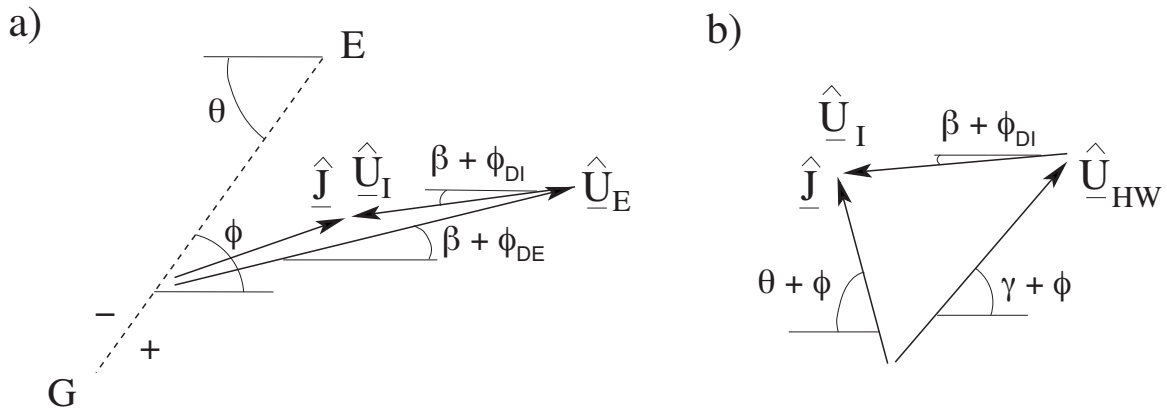

Figure 2: The hodogram of the velocity fields for the two collapse mechanisms presented in Figure 1.

$$\frac{\hat{J}}{\sin(\phi_{DE}-\phi_{DI})} = \frac{1}{\sin(\theta-\phi-\beta-\phi_{DE})} = \frac{\hat{U}_E}{\sin(\theta-\phi-\beta-\phi_{DI})}\,, \tag{17}$$

with obvious constraints on the three internal angles.

The internal region of the velocity field for the second collapse mechanisms is the same as in (16). The external region is at rest and the motion of the rear part of the wedge is accommodated by two faults GE and GF, typical of a thrust fold. The velocity of the hanging wall $\underline{\hat{U}}_{HW}$ is oriented at ϕ from the ramp GE dipping at γ:

$$\underline{\hat{U}}_{HW} = \hat{U}_{HW}\Big(\cos(\gamma+\phi)\underline{e}_1 + \ sin(\gamma+\phi)\underline{e}_2\Big)\,. \tag{18}$$

The difference between this velocity and the internal velocity is the jump across the fault GF dipping at θ. This jump has an unknown norm $\hat{J}$ and is orientated at ϕ from the fault. The construction of this velocity field is illustrated by the hodogram in Figure 2b. Application of the rule of sines to this second triangular construction provides:

$$\frac{\hat{U}_{HW}}{\sin(\beta+\phi_{DI}+\theta+\phi)} = \frac{1}{\sin(\gamma+\theta+2\phi)} = \frac{\hat{J}}{\sin(\gamma+\phi-\beta-\phi_{DI})}\,. \tag{19}$$

These conditions define entirely the velocity fields of the two collapse mechanisms for a given orientation of the fault GE (θ) and of the two faults GE and GF (θ and γ) for the first and the second collapse mechanism, respectively. Application of (15) to get the upper bound for each mechanism is then rather straight forward. These upper bounds are then minimized to obtain the least upper bound by varying θ or θ and γ depending on the collapse mechanism. This minimization is done numerically following the method discussed in Cubas et al. [2008]. The least of the two minimized upper bounds determines the dominant collapse mechanism.

References

Chandrasekharaiah D.S. and L. Debnath (1994). Continuum Mechanics, Publisher: Academic press, Inc.

Cubas, N., Barnes, C., Maillot B. (subm.b), Inverse method applied to a sand wedge: estimation of friction parameters and uncertainty analysis.

Cubas, N., J.P. Avouac, P. Souloumiac and Y.M. Leroy (subm.a), Megathrust friction determined from mechanical analysis of the forearc in the Maule Earthquake area.

Cubas, N., Y.M. Leroy and B. Maillot (2008), Prediction of thrusting sequences in accretionary wedges, *J. of Geophys. Res.*, v.113, p.1-21.

Dahlen, F. A. (1984), Noncohesive Critical Coulomb Wedges: An Exact Solution, *J. of Geophys. Res.*, v.89,

p.10125-10133.
Hubbert, M., Rubey, W. (1959), Role of the fluid pressure in mechanics of overthrust faulting, 1, Mechanics of fluid-filled solids and its application to overthrust faulting, *Geological Society of America Bulletin*, v.70, p.115-166.
Maillot, B., and Y.M. Leroy (2006), Kink-fold onset and development based on the maximum strength theorem, *J. of the Mech. and Physics of Solids*, v.54, p.2030-2059.
Pons, A., Y. M. Leroy, S. Lallemant (2013), Fluid pressure control on splay fault activation in accretionary prism based on the maximum strength theorem with application to the Nankai wedge, Earth and Planetary Science Letters, v. 368, p.4350, DOI:10.1016/j.epsl.2013.02.038.
Pons, A. and Y.M. Leroy (2012), Stability of accretionary wedges based on the maximum strength theorem for fluid-saturated porous media, *J. of the Mech. and Physics of Solids*, v.60, p.643-664, doi:10.1016/j.jmps.2011.12.011.
Salençon, J. (2002), De lElasto-Plasticité au Calcul à la Rupture, Ellipses, Paris, 264p.
Souloumiac, P., Y. M. Leroy, B. Maillot and K. Krabbenhoft (2009), Predicting stress distributions in fold-and-thrust belts and accretionary wedges by optimization, J. Geophys. Res., v.114, doi:10.1029/2008JB005986.